Received: 22 August 2022 | Revised: 24 September 2022 | Accepted: 26 September 2022

DOI: 10.1002/poc.4447

RESEARCH ARTICLE

Journal of Physical Organic Chemistry WILEY

In the quest of Hückel–Hückel and Hückel–Baird double aromatic tropylium (tri)cation and anion derivatives

Sílvia Escayola[1,2] | **Nathalie Proos Vedin**[3] | **Albert Poater**[1] | **Henrik Ottosson**[3] | **Miquel Solà**[1]

[1]Institut de Química Computacional i Catàlisi and Departament de Química, Universitat de Girona, C/ Maria Aurèlia Capmany, 69, Girona, Catalonia, 17003, Spain

[2]Donostia International Physics Center (DIPC), Manuel Lardizabal Ibilbidea, 4, Donostia, Euskadi, 20018, Spain

[3]Department of Chemistry - Ångström Laboratory, Uppsala University, Lägerhyddsvägen, 1, Uppsala, 75120, Sweden

Correspondence
Henrik Ottosson, Department of Chemistry - Ångström Laboratory, Uppsala University, 75120 Uppsala, Sweden.
Email: henrik.ottosson@kemi.uu.se

Miquel Solà, Institut de Química Computacional i Catàlisi and Departament de Química, Universitat de Girona, C/ Maria Aurèlia Capmany, 69, 17003 Girona, Catalonia, Spain.
Email: miquel.sola@udg.edu

Funding information
Generalitat de Catalunya, Grant/Award Number: 2017SGR39; Ministerio de Ciencia e Innovación, Grant/Award Numbers: PID2020-113711GB-I00, PID2021-127423NB-I00; Swedish Research Council, Grant/Award Number: 2019-05618; Universitat de Girona, Grant/Award Number: IFUdG2019; Swedish National Infrastructure for Computing

Abstract

Besides the most common form of aromaticity involving a π-ring, hexaiodobenzene and hexakis(phenylselenyl)benzene dications also present σ-aromaticity in the outer ring formed by the main group substituents. These two compounds are considered σ- and π-double aromatic, and their characterization is of special interest to the fields of organic and structural chemistry. In this work, we decided to explore the double aromaticity in substituted tropylium cations for three reasons: (i) the seven neutral halogen substituents of the tropylium cations will, without oxidation, lead to 14 σ-electrons (a $4n + 2$ Hückel number); (ii) tropylium cations are highly stable and can be easily generated experimentally; and (iii) whereas in substituted benzenes the distances between substituents in the optimized structures or X-ray crystals are too large to allow strong σ-aromaticity, these distances are expected to be shorter in substituted tropylium cations. Yet, instead of the expected σ-aromaticity, we found that the most stable geometries are highly puckered, meaning that delocalization in both π- and σ-systems is lost. Our results, which include also the tropylium anion and trication in the singlet and triplet state, show that there is a need to open a lone pair hole by oxidation to generate σ-aromaticity. Among the systems studied, only triplet $C_7Br_7^{+3}$ with an internal Hückel aromatic tropylium ring and an external incipient Baird aromatic Br_7 ring shows double π- and σ-aromaticity. This result, however, is functional-dependent and reveals that $^3C_7Br_7^{3+}$ is at the borderline for onset of double aromaticity.

KEYWORDS

Baird aromaticity, density functional theory, double aromaticity, excited state aromaticity, theoretical and computational chemistry

1 | INTRODUCTION

Aromaticity has been a central concept in chemistry since the discovery of benzene by Michael Faraday in 1825.[1] It has traditionally been associated with cyclic conjugated organic compounds that present a high π-electron delocalization.[2] For a long time, aromaticity was exclusively associated with π-electrons. However, already in 1979, Dewar introduced the concept of σ-aromaticity to explain the properties of cyclopropane,[3] although, much more recently, Schleyer proved that cyclopropane is not a σ-aromatic molecule.[4] The simplest aromatic molecule, H_3^+, is, in fact, a σ-aromatic molecule.[5] The first doubly aromatic system, the 3,5-dehydrophenyl cation, was identified by Schleyer and coworkers to possess σ- and π-aromaticity.[6] In recent years, the concept of aromaticity has been extended into inorganic chemistry.[7] It turns out that aromaticity in all-metal and semimetal clusters is much more complex than in organic chemistry with several possible combinations of aromaticities and antiaromaticies in the same molecule. The list of molecules with double or triple aromaticity or conflicting aromaticity is large. We briefly mention here four species: $LiAl_4^-$, which is double σ- and π-aromatic,[8] $Li_3Al_4^-$, which in the singlet state is σ-aromatic and π-antiaromatic[9] and in the triplet state is Hückel σ-aromatic and Baird π-aromatic,[10] B_6^{2-}, which is double σ- and π-antiaromatic,[11] and Hf_3, which is triple σ-, π-, and δ-aromatic.[7c,12]

Double aromaticity in classical organic chemistry is much more elusive. Cyclo[18]carbon, recently characterized by high-resolution atomic force microscope, can be considered as one such example of double Hückel π_{in} and π_{out} aromaticities.[13] Another example is the cyclo[16]carbon in its quintet state that was reported to be double Baird π_{in} and π_{out} aromatic.[14] Let us mention here that Baird's rule states that annulenes with $4n$ π-electrons are aromatic and those with $4n + 2$ are antiaromatic in their lowest triplet states.[15] In 1989, Sagl and Martin[16] synthesized the stable singlet ground state dication of hexaiodobenzene, $C_6I_6^{+2}$ (see Scheme 1A, right). Martin et al. provided much evidence on that such a dication had a double Hückel σ-aromaticity (with 10 delocalized electrons through the hexaiodo substituents) and π-aromaticity (with six delocalized electrons in the benzene ring).[16,17] Further theoretical studies supported the double σ- and π-aromaticity of the hexaiodobenzene cation.[18] Other hexahalobenzene dications and the singlet and triplet $C_6(ChH)_6^{2+}$ (Ch = S, Se, Te) species were explored computationally as potential candidates of double aromatic compounds.[19] Sundholm, Liegeois et al.[20] concluded that not only $C_6I_6^{2+}$ but also $C_6At_6^{2+}$, $C_6(SeH)_6^{2+}$, $C_6(SeMe)_6^{2+}$, $C_6(TeH)_6^{2+}$, $C_6(TeMe)_6^{2+}$, and $C_6(SbH_2)_6^{2+}$ dications are doubly aromatic sustaining spatially separated ring currents in the carbon ring and in the outer ring of the molecule. Borazine analogues of hexaiodobenzene and hexakis (selenyl)benzene dication $B_3N_3I_6^{2+}$ as well as $B_3N_3(TeH)_6^{2+}$ were also reported to be doubly aromatic.[21] Double σ- and π-aromaticity was further claimed in a synthesized bishomotriboriranide[22] and in twisted thienylene-phenylene structures in toroidal and catenated topologies.[23]

Scheme 1 shows different σ- and π-electron counting situations in hexahalo- or hexachalco-substituted benzene and tropylium species in two oxidation states. Substituted benzene (Scheme 1A, left) is Hückel π-aromatic. Despite the fact that it has 12 σ-electrons, a $4n$ number, it cannot be Baird aromatic because one cannot generate a lowest-lying triplet state within the σ-orbital framework formed by the in-plane lone-pairs of the X substituents as these orbitals are fully occupied in the singlet ground state. Doubly oxidized benzene in its singlet ground state with two electrons removed from the σ-system (Scheme 1A, right) is double Hückel σ- and π-aromatic for some X substituents (X = I, At, SeH, TeH, ...). On the other hand, the tropylium cation in its singlet ground state (Scheme 1B, left) could be hypothetically classified as Hückel aromatic in both the σ- and π-systems. Finally, doubly oxidized tropylium cation in a triplet state with two electrons removed from the σ-system and two unpaired σ-electrons could be hypothetically

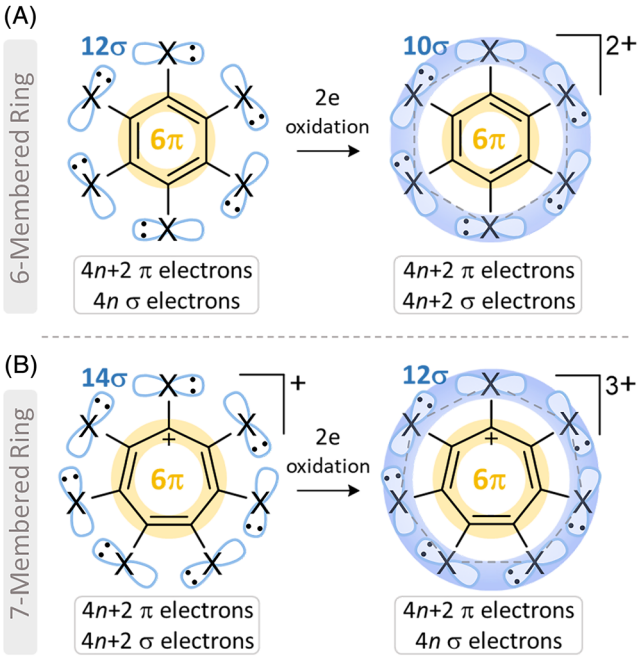

SCHEME 1 (A, B) Representation of different σ- and π-electron counting situations in hexahalo- or hexachalco-substituted (oxidized) benzene and tropylium species

Hückel π-aromatic and Baird σ-aromatic (double Hückel–Baird aromatic, Scheme 1B, right).

In 2018, Saito and co-workers reported in a combined computational and experimental study on the double σ- and π-aromatic character of the bench-stable hexakis(phenylselenyl)benzene dication (**1** in Figure 1).[24] Yet, the distance between the Se atoms in the X-ray crystal structure were 3.24–3.34 Å, and as a result, the σ-aromaticity can only be weak. Recently, with the aim to increase the overlap between the atoms of the outer cycle, Fowler and Havenith performed a computational study of the double aromaticity in larger eight-membered ring model systems $C_8I_8^q$ with charges $q = 0$, +1, +2, +4, −2.[25] However, the large I-I steric repulsion led to highly puckered structures with lack of both σ- and π-aromaticity. The authors demonstrated that in the case of planar constrained geometries with D_{4h} symmetry the systems exhibit double σ- and π-aromaticity. To our knowledge, to date no studies have been performed on substituted tropylium cations and anions (Scheme 1B and **2**, **3**, and **4** in Figure 1) as possible candidates for double σ- and π-aromaticity. Tropylium cations are especially interesting for three reasons: (i) the tropylium cations are highly stable and can be easily generated experimentally and dissolved in a variety of solvents including methanol; (ii) whereas in the case of substituted benzene the distances between substituents in the optimized structures or X-ray crystal are too large to allow strong σ-aromaticity, these distances are expected to be shorter in substituted tropylium cations, allowing for stronger through-space interaction (however, if the X–X repulsion is too strong the molecule may pucker, losing aromatic character); and (iii) the halogen substituents of the tropylium cations lead to a 14 σ-electrons, a $4n + 2$ Hückel number; that is, we can test the ability to form a σ-aromatic ring when that halogen ring-system is neutral. Apart from the heptahalotropylium cation, several other combinations with tropylium anion and trication (**3** and **4**) with expected Baird/Hückel and Hückel/Baird double aromaticities in their triplet states have been tested (see Figure 1).

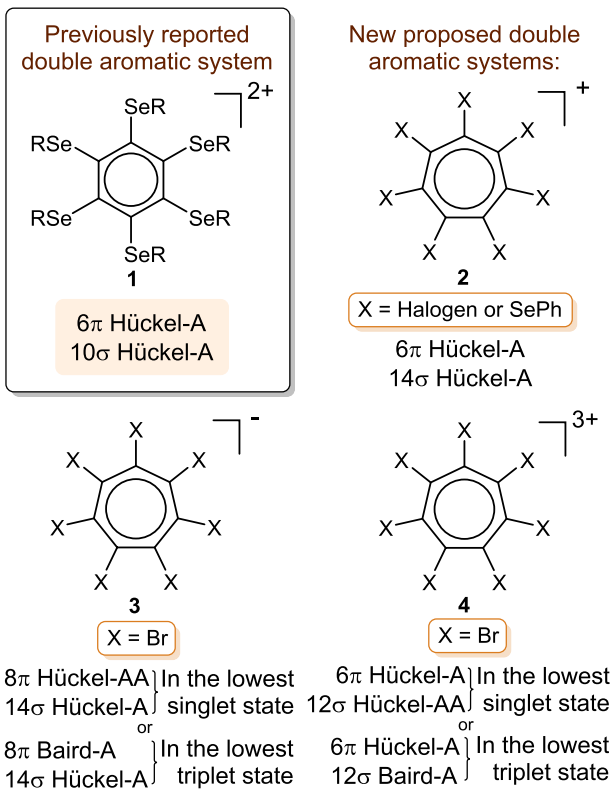

FIGURE 1 Systems with tropylium rings considered in our study (A stands for aromatic and AA for antiaromatic). In cases where the electron count leads to antiaromaticity, we expect the systems to pucker to become non-aromatic.

The ground state of the heptahalotropylium cation **2** is a singlet state that may be described by a 6π-electron Hückel-aromatic cycle and a 14σ-electron Hückel-aromatic cycle. Yet, for the heptahalotropylium anion **3**, the situation could be different as the singlet state potentially needs to be described as non-aromatic in both the 8π- and 14σ-electron cycles as the 8π-electron ring likely distorts so as to alleviate the Hückel-antiaromaticity at the D_{7h} symmetry, whereby the weak 14σ-electron Hückel aromaticity will be destroyed. In contrast, in the triplet state of **3** one can have a D_{7h} symmetric structure with a Baird-aromatic 8π-electron cycle as well as a 14σ-electron Hückel-aromatic cycle. With this investigation, we would like to answer questions such as the following: To what extent can neutral σ-electron systems sustain σ-aromaticity? Which are the limitations of double aromaticity and which general guiding rules can be given? Which state is the ground state of the heptahalotropylium anions, the singlet or the triplet?

2 | COMPUTATIONAL DETAILS

All density functional theory (DFT) calculations were performed with Gaussian 16,[26] using BLYP, which combines Becke's 1988 exchange functional with the Lee, Yang, and Parr correlation functional.[27] The electronic configuration of the H, C, F, Cl, and Br atoms was described with the 6-311+G(d,p) basis set of Pople and co-workers,[28] whereas for I atoms the small-core quasi-relativistic Stuttgart/Dresden effective core potential, with an associated valence basis set (SDD), was employed.[29] The geometry optimizations were carried out with D_{7h} (and C_2 when D_{7h} was not possible) symmetry and also without symmetry constraints, and analytical frequency calculations were computed for the

characterization of the located stationary points. It is well known that the BLYP functional exaggerates delocalization in aromatic systems.[30] In our study, we use this functional to exaggerate delocalization so as to not overlook any system that potentially could be in-plane σ-aromatic. However, to check the reliability of our results, in some particular cases, we have evaluated the performance of hybrid, B3LYP[27b,31] and M06-2X,[32] and long range corrected, CAM-B3LYP,[33] functionals (see supporting information, SI, for more details).

The aromaticity has been quantified using structural, electronic, and magnetic probes of aromaticity. As structural measure of aromaticity, the planarity root-summed-square (RSS) index[34] was used. This index measures the deviation of a selection of atoms (in our case the seven or eight C atoms—RSS_C—or the seven or eight halogen atoms—RSS_X) from the best fitted plane and it is related to the fact that small aromatic systems usually prefer to be planar. As electronic indices,[35] we employed the multicenter index (MCI)[36] and the electron density of delocalized bonds (EDDB).[37] MCI measures the electron delocalization between different centers. Because of its size dependency, when comparing MCI of rings of different sizes, it is advisable to use the normalized version, $MCI^{1/N}$, where N is the number of atoms in the ring.[38] The EDDB method decomposes the one-electron density in several "layers" corresponding to different levels of electron delocalization,[39] namely, the density of electrons localized on atoms (EDLA) representing inner shells, lone pairs, and so on; the electron density of localized bonds (EDLB) representing typical (2-center 2-electron) Lewis-like bonds; and EDDB, which represents electron density that cannot be assigned to atoms or bonds due to its (multicenter) delocalized nature. The EDDB population of electrons delocalized through the system of all conjugated bonds in a ring can be used as an indicator of aromaticity.[40] Finally, as magnetic indicator, we used the out-of-plane component of the nucleus-independent chemical shift (NICS), placing the probe at the ring plane and at 1 Å above and below it ($NICS[0, 1, \text{and } -1]_{zz}$).[41] In this case, negative values are indicative of aromatic structures, while positive values indicate non- or anti-aromaticity. In all cases, the computational level was the same as for the geometry optimization. Gaussian 16 was employed in the computation of all aromaticity and delocalization indices to get the geometry and wavefunction information used in AIMAll[42] together with ESI-3D[43] packages (for MCI), and NBO 6.0 together with the RunEDDB code for EDDB.[44]

3 | RESULTS AND DISCUSSION

This section is organized as follows. First, we discuss the results for the $C_7X_7^+$ cationic species (X = F, Cl, Br, and I); second, we analyze the singlet and triplet $C_7Br_7^-$ anionic systems; and, finally, we investigate the possibility of having double aromaticity in the singlet and triplet states of the $C_7Br_7^{+3}$ species.

3.1 | The tropylium cation derivatives

Figure 2 and Table 1 contain the most important geometric parameters of the restricted to D_{7h} symmetry and fully optimized (C_1) $C_7X_7^+$ species **2** (X = F, Cl, Br, and I) in their singlet states. As can be seen, the molecule remains planar only in the case of $C_7F_7^+$. For all other systems, the planar geometry is a transition state for ring inversion with at least two out-of-plane distortions that stabilize the molecule. Moving from D_{7h} to C_1 symmetry releases 0.0, 1.3, 8.1, and 34.4 kcal/mol for $C_7F_7^+$, $C_7Cl_7^+$, $C_7Br_7^+$, and $C_7I_7^+$, respectively. According to the RSS values of Figure 2, the loss of planarity for the X_7 ring is much larger than that for the C_7 ring. Except for X = F, the X–X lone pair repulsions are strong enough to force the molecule to pucker losing the potential σ-aromatic character. Through the distortion of the planar geometry, the X–X distance increases from 0.05 for X = Cl to 0.15 Å for X = I. Puckering is not unexpected given that (i) the angle strain in seven-membered rings (7-MRs) can promote puckering as compared to the hexagonal 6-MRs, which are ideal for sp^2 C atoms[45]; (ii) the lowest out-of-plane (oop) frequency changes from 212 cm^{-1} in planar $^1C_7H_7^+$ to 81 cm^{-1} in planar $^1C_7F_7^+$ (see Table S2), showing that increasing the size of X in $^1C_7X_7^+$ increases steric congestion that promotes puckering of the 7-MR; and

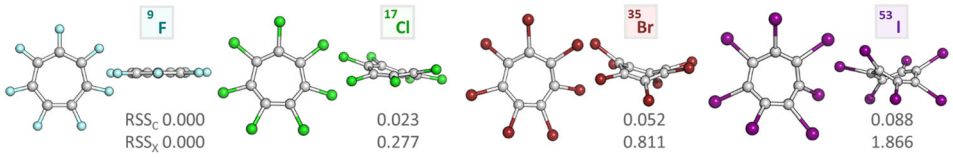

FIGURE 2 Front and side view of the fully optimized $^1C_7X_7^+$ (X = F, Cl, Br, and I) geometries using BLYP/6-311+G(d,p)∼SDD(I) and the planarity root-summed-square (RSS) index computed for the C- and X-rings (RSS_C and RSS_X, respectively)

TABLE 1 $R_{C\text{-}C}$, $R_{C\text{-}X}$, and $R_{X\text{-}X}$ distances (Å) and number of imaginary frequencies for the relaxed and D_{7h} constrained geometries of $^1C_7X_7^+$ (X = H, F, Cl, Br, and I) and $^1C_6(SePh)_6^{2+}$ and $^1C_6I_6^{2+}$ compounds optimized at the BLYP/6-311+G(d,p)~SDD (for I) level of theory

System	$R_{C\text{-}C}$	$R_{C\text{-}X}$	$R_{X\text{-}X}$	$n_{imag.}$
$^1C_6(SePh)_6^{2+}$ (D_{2h})[a]	1.402	1.959	3.353 3.358 3.364	0
$^1C_6I_6^{2+}$ (D_{6h})	1.404	2.147	3.551	0
$^1C_7H_7^+$ (D_{7h})	1.406	1.092	2.354	0
$^1C_7F_7^+$ (D_{7h})	1.412	1.326	2.562	0
$^1C_7Cl_7^+$ (D_{7h})	1.432	1.742	2.944	2 (A″)
$^1C_7Cl_7^+$ (C_1)	1.434 1.431 1.426 1.424	1.742 1.740 1.738 1.737	3.007 3.002 2.995 2.992	0
$^1C_7Br_7^+$ (D_{7h})	1.435	1.925	3.106	4 (A″)
$^1C_7Br_7^+$ (C_1)	1.442 1.440 1.436 1.428 1.423 1.415 1.412	1.921 1.919 1.917 1.912 1.909 1.905 1.903	3.290 3.284 3.278 3.263 3.256 3.248 3.247	0
$^1C_7I_7^+$ (D_{7h})	1.440	2.212	3.359	4 (A″)
$^1C_7I_7^+$ (C_1)	1.456 1.454 1.443 1.431 1.407 1.394 1.386	2.172 2.170 2.165 2.160 2.147 2.139 2.131	3.744 3.741 3.738 3.722 3.676 3.666 3.660	0

[a]Optimized geometry at B3LYP-D3/6-31G(d)~SDD level of theory obtained from previous reference.[24]

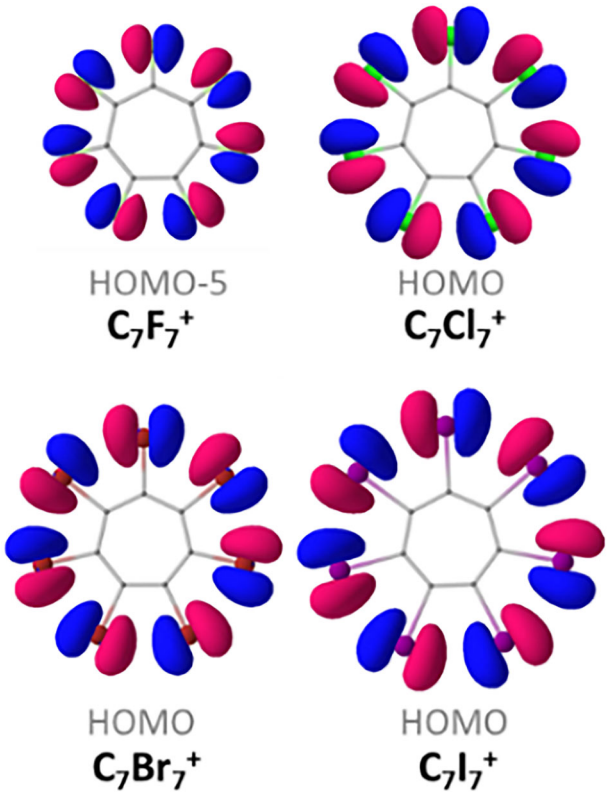

FIGURE 3 The HOMO-5 of D_{7h} $^1C_7F_7^+$ and the HOMO of D_{7h} $^1C_7X_7^+$ (X = Cl, Br, and I)

(iii) the highest occupied molecular orbital (HOMO) of D_{7h} $C_7X_7^+$ (X = Cl, Br, and I) contains seven in-plane antibonding interactions in the ring of X substituents (see Figure 3). The same type of HOMO with maximal in-plane antibonding interaction between the substituents was found by Fowler and Havenith in D_{4h} constrained C_8I_8.[25]

Interestingly, the distortion has a relatively small effect on the aromaticity of the tropylium ring, except in the case of X = I, for which the aromaticity reduction when going from D_{7h} to C_1 is more pronounced (see Table 2). This is in agreement with previous studies showing that π-aromaticity is quite robust with respect to out-of-plane and in-plane distortions.[46] Table 3 provides the aromaticity indices corresponding to the X_7 ring. As can be seen, the MCI is zero and the EDDB points to a residual delocalization in the X_7 ring, marginally larger for compounds with D_{7h} symmetry. In contrast, double aromatic $^1C_6(SePh)_6^{2+}$ and $^1C_6I_6^{2+}$ (especially the latter) have relatively large MCI_X and σ-$EDDB_X$. In the case of planar $^1C_7F_7^+$, the *2p* orbitals of F are not diffuse enough to generate σ-delocalization. For the rest of the systems, which lose planarity, MCI, EDDB values, small X–X delocalization indices (see Table S3) as well as ring currents (see Figure S6) are in agreement with lack of

System	MCI_C	σ-$EDDB_C(r)$	π-$EDDB_C(r)$	$NICS(0)_{zz}$	$NICS(1)_{zz}$
$^1C_6(SePh)_6^{2+}$ (D_{2h})[a]	0.0517	0.381	4.683	−25.0	−35.1
$^1C_6I_6^{2+}$ (D_{6h})	0.0548	0.472	4.666	−31.9	−37.3
$^1C_7H_7^+$ (D_{7h})	0.0579	0.385	5.865	−15.9	−25.6
$^1C_7F_7^+$ (D_{7h})	0.0253	0.182	4.698	−13.8	−18.3
$^1C_7Cl_7^+$ (D_{7h})	0.0228	0.306	4.397	−3.4	−12.7
$^1C_7Cl_7^+$ (C_1)	0.0221	0.274	4.228	−4.2	−12.7[b]
$^1C_7Br_7^+$ (D_{7h})	0.0238	0.406	4.505	−4.2	−12.0
$^1C_7Br_7^+$ (C_1)	0.0210	0.310	3.800	−4.0	−10.9[b]
$^1C_7I_7^+$ (D_{7h})	0.0291	0.609	4.733	18.5[c]	27.9[c]
$^1C_7I_7^+$ (C_1)	0.0168	0.432	2.548	−7.8	−11.1[b]

[a]Optimized geometry at B3LYP-D3/6-31G(d)∼SDD level of theory obtained from previous reference.[24]
[b]In the case of the non-symmetric systems the NICS(1) corresponds to the average of NICS(1) and (−1).
[c]These positive NICS values are an artifact produced by the exchange between LUMO and LUMO+2 when moving from $^1C_7Br_7^+$ (D_{7h}) to $^1C_7I_7^+$ (D_{7h}) (see Figure S2).

TABLE 2 Aromaticity indices (MCI and EDDB in electrons, NICS in ppm) corresponding to the C-ring for the relaxed and D_{7h} constrained geometries of $C_7X_7^+$ (X = H, F, Cl, Br, and I) compounds calculated at the BLYP/6-311+G(d,p)∼SDD(I) level of theory

TABLE 3 Aromaticity indices (MCI and EDDB in electrons) corresponding to the X-ring for the relaxed and D_{7h} constrained geometries of $C_7X_7^+$ (X = F, Cl, Br, and I) compounds calculated at the BLYP/6-311+G(d,p)∼SDD(I) level of theory

System	MCI_X	σ-$EDDB_X(r)$	π-$EDDB_X(r)$
$^1C_6(SePh)_6^{2+}$ (D_{2h})[a]	0.0055	2.923	0.062
$^1C_6I_6^{2+}$ (D_{6h})	0.0444	5.251	0.087
$^1C_7F_7^+$ (D_{7h})	0.0000	0.103	0.200
$^1C_7Cl_7^+$ (D_{7h})	0.0000	0.210	0.338
$^1C_7Cl_7^+$ (C_1)	0.0000	0.201	0.301
$^1C_7Br_7^+$ (D_{7h})	0.0000	0.217	0.379
$^1C_7Br_7^+$ (C_1)	0.0000	0.230	0.324
$^1C_7I_7^+$ (D_{7h})	0.0000	0.180	0.462
$^1C_7I_7^+$ (C_1)	0.0000	0.299	0.301

[a]Optimized geometry at B3LYP-D3/6-31G(d)∼SDD level of theory obtained from previous reference.[24]

σ-aromaticity in $C_7X_7^+$ (X = Cl, Br, and I). The above statement, is reinforced when we compare the MCI and EDDB values (Table 3) of $^1C_7X_7^+$ with $^1C_6(SePh)_6^{2+}$, previously characterized as weakly σ-aromatic, observing that the latter are more than an order of magnitude higher. As to the π-aromaticity, such aromaticity is found in the D_{7h} species and is reduced somewhat when going to the final optimized species. As a whole, despite having a favorable electron counting (Figure 1), $C_7X_7^+$ (X = F, Cl, Br, and I) species are not double σ- and π-aromatic, they are simply π-aromatic. Finally, let us mention that we obtained unexpected positive NICS values for $C_7I_7^+$. These positive NICS values are an artifact produced by the exchange between LUMO and LUMO+2 when moving from $^1C_7Br_7^+$ (D_{7h}) to $^1C_7I_7^+$ (D_{7h}) (see Figure S2) that results in a change in the direction of the ring current that becomes paramagnetic (see Figure S6), thus explaining the positive NICS values. This is another example of the fact that there is not always a correspondence between ring currents and aromaticity.[47] Since NICS failures are more common in open-shell species,[48] we decided not to include NICS values in the discussion of the coming sections.

3.2 | The tropylium anion derivatives

Next, we decided to analyze compound **3** for X = Br, $C_7Br_7^-$, in the singlet and triplet states. In the singlet state, with 8π-electrons, we do not expect aromaticity in the tropylium ring. For the triplet state, however, it is possible to have Baird π-aromaticity in the tropylium ring and Hückel σ-aromaticity in the external ring through the Br_7 ring (14σ-electrons). We limited our study to $^1C_7Br_7^-$ and $^3C_7Br_7^-$ for two reasons: (i) X = Br is preferred over X = I to avoid excessive steric congestion that will result in ring puckering and (ii) X = Br is preferred to X = Cl because the Br atom has more diffuse *4p* orbitals that can lead to better overlaps. In the case of the triplet state, the D_{7h} optimization was not possible and instead a planar C_2 optimized geometry was obtained. Going from planar to puckered $C_7Br_7^-$, the molecule is stabilized by 47.2 kcal/mol in the singlet state and by 18.6 kcal/mol in the triplet state. As expected, the stabilization due to puckering in the singlet state is larger because of the release of antiaromaticity when going from planar to puckered structure. According to the RSS values of Table 4, the loss of planarity for the Br_7 ring is

much larger than that of the C_7 ring. When going from the planar to the non-planar structure, the C–C bond length alternation increases and the Br–Br distance increases by 0.3–0.5 Å.

Taking the values of $^1C_7Br_7^+$ (D_{7h}) in Table 2 as reference, the MCI_C and the π-$EDDB_C(\mathbf{r})$ of the C_7 ring of $^1C_7Br_7^-$ (D_{7h}) in Table 5 are somewhat higher than that of $^1C_7Br_7^+$ (D_{7h}). QTAIM charges in the Br_7 ring of $^1C_7Br_7^+$ (D_{7h}) and $^1C_7Br_7^-$ (D_{7h}) are 1.035 and −1.183 electrons, respectively (see Table S11). Therefore, the two added extra electrons in $^1C_7Br_7^-$ (D_{7h}) are mainly located in the Br atoms. This is why the MCI_C and the π-$EDDB_C(\mathbf{r})$ of the C_7 ring of $^1C_7Br_7^+$ (D_{7h}) and $^1C_7Br_7^-$ (D_{7h}) are similar. Now, moving from D_{7h} $^1C_7Br_7^-$ to C_1 $^1C_7Br_7^-$, MCI and π-$EDDB_C(\mathbf{r})$ decrease due to the increase in the bond length alternation that results in higher π-electron localization. When going from $^1C_7Br_7^-$ (D_{7h}) to $^3C_7Br_7^-$ (C_2), MCI and π-$EDDB_C(\mathbf{r})$ point to a decrease that we attribute to the loss of symmetry and increase in the bond length alternation that leads to a greater π-electron localization. Spin density of $^3C_7Br_7^-$ (C_2) shows that the excess of spin α is distributed among the C_7 and Br_7 rings (see Figure 4). Therefore, the planar C_7 ring cannot be considered fully Baird aromatic. Finally, release of the planarity in $^3C_7Br_7^-$ leads to further reduction of the MCI and π-$EDDB_C(\mathbf{r})$.

TABLE 4 $R_{C\text{-}C}$, $R_{C\text{-}Br}$, and $R_{Br\text{-}Br}$ distances (Å), RSS, and number of imaginary frequencies for the relaxed and D_{7h} (C_2) constrained geometries in the singlet and triplet states of $C_7Br_7^-$ optimized at the BLYP/6-311+G(d,p) level of theory

System	$R_{C\text{-}C}$ (Å)	$R_{C\text{-}Br}$ (Å)	$R_{Br\text{-}Br}$ (Å)	RSS_C	RSS_{Br}	$N_{imag.}$
$^1C_7Br_7^-$ (D_{7h})	1.393	2.114	3.228	0.000	0.000	4(A″)
$^1C_7Br_7^-$ (C_1)	1.391 1.429 1.360 1.451	2.053 1.970 2.030 1.990	3.505 3.578 3.459 3.641	0.077	1.707	0
$^3C_7Br_7^-$ (C_2)	1.374 1.404 1.443 1.461	2.036 2.044 2.049	3.186 3.188 3.190 3.191	0.000	0.000	4(A″) 1(A′)
$^3C_7Br_7^-$ (C_1)	1.396 1.415 1.400 1.358 1.447 1.371 1.422	1.979 1.967 2.428 1.980 1.972 2.073 2.003	3.488 3.459 3.780 3.618 3.462 3.431 3.716	0.061	1.601	0

TABLE 5 Aromaticity indices (MCI and EDDB in electrons) corresponding to the C-ring for the relaxed (C_1) and constrained (D_{7h} or C_2) geometries in the singlet and triplet states of $C_7Br_7^-$ computed at the BLYP/6-311+G(d,p) level of theory

System	MCI_C	σ-$EDDB_C(\mathbf{r})$	π-$EDDB_C(\mathbf{r})$
$^1C_7Br_7^-$ (D_{7h})	0.0381	1.168	4.924
$^1C_7Br_7^-$ (C_1)	0.0080	0.477	2.327
$^3C_7Br_7^-$ (C_2)	0.0172	0.711	3.530
$^3C_7Br_7^-$ (C_1)	0.0121	1.119	2.336

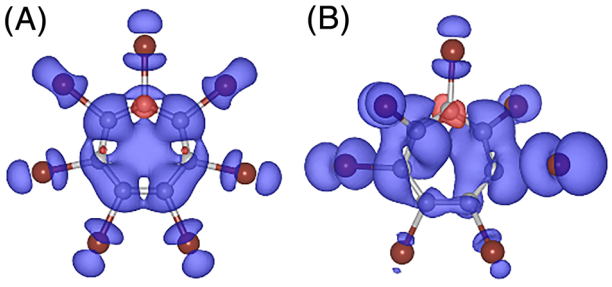

FIGURE 4 Spin density distribution of (A) C_2 and (B) C_1 $^3C_7Br_7^-$. The isodensity corresponds to a value of 0.002 $e^-/bohr^3$. The positive and negative spin densities are represented in blue and red, respectively.

The loss of planarity, the low MCI and EDDB values in Table 6, and the delocalization indices (see Table S4) are in agreement with lack of σ-aromaticity in the Br_7 ring of $^1C_7Br_7^-$ and $^3C_7Br_7^-$. In summary, neither $^1C_7Br_7^-$ nor $^3C_7Br_7^-$, the latter despite having a favorable electron counting for Baird π- and Hückel σ-aromaticity, are double σ- and π-aromatic.

3.3 | The tropylium trication derivatives

As shown in previous subsections, following Hückel or Baird electron counting rules does not warrant the existence of double aromaticity. As pointed out by Schleyer et al.,[41b] aromaticity requires electron delocalization in closed circuits. In the Valence Bond language, this means that we must have a number of resonance structures with same or similar weights. In $C_7X_7^+$, we have seven resonance structures of the same weight, the resonating electrons being the 6π-electrons of the tropylium ring. However, the σ-electrons of the external electrons of X_7 ring are non-resonant localized lone pairs. Without the delocalization of the σ-electrons, in general, the systems cannot be σ-aromatic and they are only π-aromatic. Therefore, not only must the electron counting rules be fulfilled but also the σ-electrons in the external ring have to be delocalized. For instance, in the double aromatic $C_6I_6^{+2}$, double oxidation of C_6I_6 opens a hole in one of the *5p* orbitals of iodine that generates six possible resonance structures (Scheme 2 shows only three) that have the same weight. The existence of these resonance structures and the fulfillment of the Hückel's rule generate the double σ- and π-aromaticity.

TABLE 6 Aromaticity indices (MCI and EDDB in electrons) corresponding to the Br-ring for the relaxed (C_1) and constrained (D_{7h} or C_2) geometries in the singlet and triplet states of $C_7Br_7^-$ computed at the BLYP/6-311+G(d,p) level of theory

System	MCI_{Br}	σ-$EDDB_{Br}$(r)	π-$EDDB_{Br}$(r)
$^1C_7Br_7^-$ (D_{7h})	0.0003	0.742	0.236
$^1C_7Br_7^-$ (C_1)	0.0000	0.180	0.136
$^3C_7Br_7^-$ (C_2)	0.0002	0.406	0.165
$^3C_7Br_7^-$ (C_1)	0.0000	0.091	0.314

With this idea in mind, we decided to explore the singlet and triplet $C_7Br_7^{+3}$ species (system **4** in Figure 1). We expect that double oxidation of $C_7Br_7^+$ to generate $C_7Br_7^{+3}$ will create the necessary σ-delocalization. For the singlet, with 6π-electrons we expect Hückel aromaticity of the tropylium ring and Hückel antiaromaticity from the 12σ-electrons of the external Br_7 ring. On the other hand, for the triplet, we could have Hückel aromaticity of the tropylium ring and Baird aromaticity from the 12σ-electrons (10 paired and two unpaired electrons) of the outer Br_7 ring.

Interestingly, the $^1C_7Br_7^{+3}$ species is the first of our studied systems (except $^1C_7F_7^+$) that keeps the planarity and the D_{7h} symmetry (see Table 7). For the D_{7h} triplet, we have been unable to converge the self-consistent field (SCF) procedure; this was only possible for the C_2 symmetry. However, we have found a $^3C_7Br_7^{+3}$ species of C_1 symmetry that it is very close to the D_{7h} symmetry, with minor bond length alternation and RSS_C and RSS_{Br} close to zero. The energy difference with respect the C_2 constrained geometry is insignificant, only 0.03 kcal/mol. The singlet is more stable than the triplet by only 13.3 kcal/mol. These two species are good candidates to have both π-aromaticity and σ-(anti)aromaticity.

The MCI and EDDB results of $^1C_7Br_7^{+3}$ and $^3C_7Br_7^{+3}$ in Table 8 are almost identical to those of $^1C_7Br_7^+$, thus confirming the π-aromatic character of the tropylium ring in both states. Indeed, the spin density of Figure 5 is fully located in the outer Br_7 ring. On the other hand, the MCI and EDDB results of Table 9 point out the antiaromatic character of the Br_7 ring in the $^1C_7Br_7^{+3}$ species with a negative and relatively large MCI value. To our knowledge, this is the first example of an organic molecule showing conflicting aromaticity. The aromatic character of the Br_7 ring in C_1 $^3C_7Br_7^{+3}$ with a low MCI value is weak. Still this MCI value is the largest among the series of analyzed systems and is comparable to that of $C_6(SePh)_6^{2+}$ ($MCI_{Br}{}^{1/7} = 0.583$ as compared to $MCI_{Se}{}^{1/6} = 0.420$ of $C_6(SePh)_6^{2+}$). In addition, the high stability of the triplet with respect to the singlet is in agreement with the change from antiaromatic to aromatic character of the Br_7 ring when moving from the singlet to the triplet $C_7Br_7^{+3}$. Unfortunately, this double aromaticity is not confirmed by ring currents because of the high paratropic ring currents shown by the β

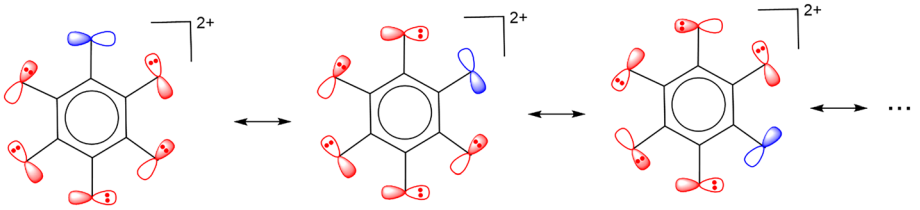

SCHEME 2 The double aromaticity in $C_6I_6^{2+}$ and similar species requires the opening of an electronic hole to generate σ-delocalization as indicated by the different resonance structures.

TABLE 7 $R_{C\text{-}C}$, $R_{C\text{-}X}$, and $R_{X\text{-}X}$ distances (Å), RSS, and number of imaginary frequencies for the relaxed and D_{7h} constrained geometries in the singlet and triplet states of $C_7Br_7^{+3}$ optimized at BLYP/6-311+G(d,p) level of theory

System	$R_{C\text{-}C}$ (Å)	$R_{C\text{-}X}$ (Å)	$R_{X\text{-}X}$ (Å)	RSS_C	RSS_{Br}	$N_{imag.}$
$^1C_7Br_7^{+3}$ (D_{7h})	1.419	1.914	3.080	0.000	0.000	0
$^3C_7Br_7^{+3}$ (C_2)	1.416 1.419 1.425 1.426	1.910 1.924 1.932 1.937	2.965 2.998 3.101 3.237	0.000	0.000	1
$^3C_7Br_7^{+3}$ (C_1)	1.426 1.418 1.421 1.426 1.424 1.416	1.908 1.926 1.936 1.920 1.913 1.933 1.930	3.206 2.984 3.018 3.250 3.074 2.968 3.146	0.001	0.008	0

TABLE 8 Aromaticity indices (MCI and EDDB in electrons) corresponding to the C-ring for the relaxed (C_1) and constrained (D_{7h} or C_2) geometries in the singlet and triplet states of $C_7Br_7^{+3}$ computed at BLYP/6-311+G(d,p) level of theory

System	MCI_C	$\sigma\text{-EDDB}_C(r)$	$\pi\text{-EDDB}_C(r)$
$^1C_7Br_7^{+3}$ (D_{7h})	0.0247	0.477	4.442
$^3C_7Br_7^{+3}$ (C_2)	0.0247	0.427	4.458
$^3C_7Br_7^{+3}$ (C_1)	0.0246	0.541	4.303

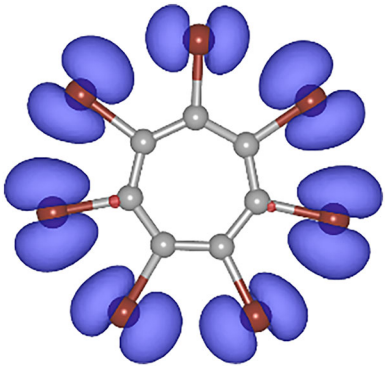

FIGURE 5 Spin density distribution of $^3C_7Br_7^{+3}$. The isodensity corresponds to a value of 0.002 $e^-/bohr^3$. The positive and negative spin densities are represented in blue and red, respectively.

TABLE 9 Aromaticity indices (MCI and EDDB in electrons) corresponding to the Br^7-ring in the singlet and triplet states of $C_7Br_7^{+3}$ computed at BLYP/6-311+G(d,p) level of theory

System	MCI_{Br}	$\sigma\text{-EDDB}_{Br}(r)$	$\pi\text{-EDDB}_{Br}(r)$
$^1C_7Br_7^{+3}$ (D_{7h})	−0.0246	5.484	0.440
$^3C_7Br_7^{+3}$ (C_2)	0.0027	2.787	0.519
$^3C_7Br_7^{+3}$ (C_1)	0.0023	2.626	0.489

electrons in $^3C_7Br_7^{+3}$ (see Figure S7). Still, we think that the results based on electron delocalization measures are more reliable than those derived from magnetic measures.

Finally, as discussed in Section 2, BLYP functional exaggerates delocalization in aromatic systems. Therefore, we expect the lack of double aromaticity in $^1C_7Br_7^+$, $^1C_7Br_7^-$, and $^3C_7Br_7^-$ to be confirmed with the B3LYP or CAM-B3LYP functionals. Less clear is the situation in triplet $C_7Br_7^{+3}$. Indeed, results obtained at the CAM-B3LYP/6-311+G(d,p) level of theory suggest that $^3C_7Br_7^{+3}$ has only π-aromaticity (see Tables S11 and S12). On the other hand, B3LYP results ($MCI_{Br}^{1/7} = 0.296$ and $\sigma\text{-EDDB}_{Br}(\mathbf{r}) = 2.313$) are intermediate between those of BLYP and CAM-B3LYP.

In summary, we have found that, first, $^{1}C_7Br_7^{+3}$ species has conflicting aromaticity,[7a,9] with an internal Hückel aromatic tropylium ring and an external Hückel antiaromatic Br_7 ring; and second, $^{3}C_7Br_7^{+3}$ has double aromaticity with an internal Hückel π-aromatic tropylium ring and an external weak Baird σ-aromatic Br_7 ring. The presence of double aromaticity in triplet $C_7Br_7^{+3}$, however, depends on the functional used. It is likely that same situation is experienced by most of the so far reported double aromatic compounds.

4 | CONCLUSIONS

Double aromatic classical organic molecules follow two requirements: (i) they must have an electron counting corresponding to the Hückel or Baird rule for both the σ- and the π-systems and (ii) they must have σ- and the π-electron delocalization that in the valence bond language means they need to have more than a single resonance structure to correctly represent the σ- and the π-electron density. These are two necessary but not sufficient conditions. The presence of strong electronic repulsion between the external substituents or substituents with *np* orbitals that are not diffuse enough may quench the σ-aromaticity by puckering the benzene or tropylium cation rings. Among the species analyzed, the most interesting ones are $^{1}C_7Br_7^{+3}$, which according to BLYP results has an internal Hückel aromatic tropylium ring and an external Hückel antiaromatic Br_7 ring, and $^{3}C_7Br_7^{+3}$ with an internal Hückel aromatic tropylium ring and an external weak Baird aromatic Br_7 ring. This result, however, is not confirmed by the B3LYP and CAM-B3LYP functionals. Yet, the functional dependent results on $^{3}C_7Br_7^{3+}$ indicate that this species is at the borderline for double aromaticity, and it reveals the importance of balancing a number of factors in the design of double aromatic molecules: (*i*) the size of the substituents should allow for close through-space contacts but not overcrowding, (*ii*) the orbital occupancies should be such that orbitals with maximal antibonding in-plane interactions between the substituents must not be occupied (achieved by oxidation), and (*iii*) the inherent angle strain of a compound, which promotes puckering of the carbon framework, should be as low as possible. Hence, for 8-MRs one needs tetraoxidation to achieve double aromaticity,[25] with 7-MRs it is achieved for the trication, and with 6-MRs it is dications that can exhibit double aromaticity.[24]

ACKNOWLEDGEMENTS

We thank the Spanish Ministerio de Ciencia e Innovación for projects PID2020-113711GB-I00 and PID2021-127423NB-I00, the Generalitat de Catalunya for project 2017SGR39, and the Swedish Research Council for project 2019-05618. A.P. is a Serra Húnter Fellow and ICREA Academia Prize 2019. S.E. thanks Universitat de Girona and DIPC for an IFUdG2019 PhD fellowship. The computations were in part enabled by resources provided by the Swedish National Infrastructure for Computing (SNIC) at the National Supercomputer Center (NSC), Linköping, Sweden.

DATA AVAILABILITY STATEMENT

A data set collection of computational results (Cartesian coordinates, energies, molecular orbitals, etc.) from this work is available in the ioChem-BD repository[49] and can be accessed via https://doi.org/10.19061/iochem-bd-4-43

ORCID

Nathalie Proos Vedin https://orcid.org/0000-0002-9313-3739
Henrik Ottosson https://orcid.org/0000-0001-8076-1165
Miquel Solà https://orcid.org/0000-0002-1917-7450

REFERENCES

[1] M. Faraday, *Philos. Trans. R. Soc. London* **1825**, *115*, 440.
[2] a) Aromaticity, *Modern computational methods and applications*, 1st ed., Elsevier, Dordrecht **2021**; b) M. Solà, A. I. Boldyrev, M. C. Cyrański, T. M. Krygowski, G. Merino, *Aromaticity and Antiaromaticity: Concepts and applications*, Wiley-VCH, Chichester **2022**.
[3] M. J. S. Dewar, *Bull. Soc. Chim. Belg.* **1979**, *88*, 957.
[4] W. Wu, B. Ma, J. I-Chia Wu, P. R. Schleyer, Y. Mo, *Chem. – Eur. J.* **2009**, *15*, 9730.
[5] R. W. A. Havenith, F. De Proft, P. W. Fowler, P. Geerlings, *Chem. Phys. Lett.* **2005**, *407*, 391.
[6] J. Chandrasekhar, E. D. Jemmis, P. V. R. Schleyer, *Tetrahedron Lett.* **1979**, *20*, 3707.
[7] a) A. I. Boldyrev, L.-S. Wang, *Chem. Rev.* **2005**, *105*, 3716; b) C. A. Tsipis, *Coord. Chem. Rev.* **2005**, *249*, 2740; c) F. Feixas, E. Matito, J. Poater, M. Solà, *WIREs Comput. Mol. Sci.* **2013**, *3*, 105.
[8] X. Li, A. E. Kuznetsov, H.-F. Zhang, A. Boldyrev, L.-S. Wang, *Science* **2001**, *291*, 859.
[9] A. E. Kuznetsov, K. A. Birch, A. I. Boldyrev, H.-J. Zhai, L.-S. Wang, *Science* **2003**, *300*, 622.
[10] D. Chen, D. W. Szczepanik, J. Zhu, M. Solà, *Chem. Commun.* **2020**, *56*, 12522.
[11] a) D. Y. Zubarev, A. I. Boldyrev, *Phys. Chem. Chem. Phys.* **2008**, *10*, 5207; b) A. N. Alexandrova, A. I. Boldyrev, H.-J. Zhai, L.-S. Wang, E. Steiner, P. W. Fowler, *J. Phys. Chem. A* **2003**, *107*, 1359.
[12] B. B. Averkiev, A. I. Boldyrev, *J. Phys. Chem. A* **2007**, *111*, 12864.
[13] K. Kaiser, L. M. Scriven, F. Schulz, P. Gawel, L. Gross, H. L. Anderson, *Science* **2019**, *365*, 1299.
[14] D. E. Bean, P. W. Fowler, A. Soncini, *Chem. Phys. Lett.* **2009**, *483*, 193.

[15] N. C. Baird, *J. Am. Chem. Soc.* **1972**, *94*, 4941.
[16] D. J. Sagl, J. C. Martin, *J. Am. Chem. Soc.* **1988**, *110*, 5827.
[17] J. C. Martin, L. J. Schaad, *Pure Appl. Chem.* **1990**, *62*, 547.
[18] I. Ciofini, P. P. Lainé, C. Adamo, *Chem. Phys. Lett.* **2007**, *435*, 171.
[19] a) M. Hatanaka, M. Saito, M. Fujita, K. Morokuma, *J. Org. Chem.* **2014**, *79*, 2640; (b) M. Orozco-Ic, J. Barroso, R. Islas, G. Merino, *ChemistryOpen* **2020**, *9*, 657.
[20] M. Rauhalahti, S. Taubert, D. Sundholm, V. Liégeois, *Phys. Chem. Chem. Phys.* **2017**, *19*, 7124.
[21] R. Pino-Rios, A. Vásquez-Espinal, O. Yañez, W. Tiznado, *RSC Adv.* **2020**, *10*, 29705.
[22] M. Unverzagt, G. Subramanian, M. Hofmann, P. v. R. Schleyer, S. Berger, K. Harms, W. Massa, A. Berndt, *Angew. Chem. Int. Ed. Engl.* **1997**, *36*, 1469.
[23] T. D. Leitner, Y. Gmeinder, F. Röhricht, R. Herges, E. Mena-Osteritz, P. Bäuerle, *Eur. J. Org. Chem.* **2020**, *2020*, 285.
[24] S. Furukawa, M. Fujita, Y. Kanatomi, M. Minoura, M. Hatanaka, K. Morokuma, K. Ishimura, M. Saito, *Commun. Chem.* **2018**, *1*, 60.
[25] P. W. Fowler, R. W. A. Havenith, *J. Phys. Chem. A* **2021**, *125*, 6374.
[26] M. J. Frisch, G. W. Trucks, H. B. Schlegel, G. E. Scuseria, M. A. Robb, J. R. Cheeseman, G. Scalmani, V. Barone, G. A. Petersson, H. Nakatsuji, X. Li, M. Caricato, A. V. Marenich, J. Bloino, B. G. Janesko, R. Gomperts, B. Mennucci, H. P. Hratchian, J. V. Ortiz, A. F. Izmaylov, J. L. Sonnenberg, F. Ding Williams, F. Lipparini, F. Egidi, J. Goings, B. Peng, A. Petrone, T. Henderson, D. Ranasinghe, V. G. Zakrzewski, J. Gao, N. Rega, G. Zheng, W. Liang, M. Hada, M. Ehara, K. Toyota, R. Fukuda, J. Hasegawa, M. Ishida, T. Nakajima, Y. Honda, O. Kitao, H. Nakai, T. Vreven, K. Throssell, J. A. Montgomery Jr., J. E. Peralta, F. Ogliaro, M. J. Bearpark, J. J. Heyd, E. N. Brothers, K. N. Kudin, V. N. Staroverov, T. A. Keith, R. Kobayashi, J. Normand, K. Raghavachari, A. P. Rendell, J. C. Burant, S. S. Iyengar, J. Tomasi, M. Cossi, J. M. Millam, M. Klene, C. Adamo, R. Cammi, J. W. Ochterski, R. L. Martin, K. Morokuma, O. Farkas, J. B. Foresman, D. J. Fox, Gaussian 16 Rev. B.01, Wallingford, CT, **2016**.
[27] a) A. D. Becke, *Phys. Rev. A* **1988**, *38*, 3098; b) C. Lee, W. Yang, R. G. Parr, *Phys. Rev. B* **1988**, *37*, 785.
[28] a) R. Krishnan, J. S. Binkley, R. Seeger, J. A. Pople, *J. Chem. Phys.* **1980**, *72*, 650; b) T. Clark, J. Chandrasekhar, G. W. Spitznagel, P. v. R. Schleyer, *J. Comput. Chem.* **1983**, *4*, 294.
[29] a) U. Häussermann, M. Dolg, H. Stoll, H. Preuss, P. Schwerdtfeger, R. M. Pitzer, *Mol. Phys.* **1993**, *78*, 1211; b) T. Leininger, A. Nicklass, H. Stoll, M. Dolg, P. Schwerdtfeger, *J. Chem. Phys.* **1996**, *105*, 1052.
[30] a) D. W. Szczepanik, M. Solà, M. Andrzejak, B. Pawelek, J. Dominikowska, M. Kukulka, K. Dyduch, T. M. Krygowski, H. Szatylowicz, *J. Comput. Chem.* **2017**, *38*, 1640; b) I. Casademont-Reig, R. Guerrero-Avilés, E. Ramos-Cordoba, M. Torrent-Sucarrat, E. Matito, *Angew. Chem., Int. Ed.* **2021**, *60*, 24080;
[31] a) A. D. Becke, *J. Chem. Phys.* **1993**, *98*, 5648; b) P. J. Stephens, F. J. Devlin, C. F. Chabalowski, M. J. Frisch, *J. Phys. Chem.* **1994**, *98*, 11623.
[32] Y. Zhao, D. G. Truhlar, *Theor. Chem. Acc.* **2008**, *120*, 215.
[33] T. Yanai, D. P. Tew, N. C. Handy, *Chem. Phys. Lett.* **2004**, *393*, 51.
[34] E. Matito, J. Poater, M. Duran, M. Solà, *J. Mol. Struct.: THEOCHEM* **2005**, *727*, 165.
[35] F. Feixas, E. Matito, J. Poater, M. Solà, *Chem. Soc. Rev.* **2015**, *44*, 6434.
[36] P. Bultinck, R. Ponec, S. Van Damme, *J. Phys. Org. Chem.* **2005**, *18*, 706.
[37] D. W. Szczepanik, M. Andrzejak, J. Dominikowska, B. Pawełek, T. M. Krygowski, H. Szatylowicz, M. Solà, *Phys. Chem. Chem. Phys.* **2017**, *19*, 28970.
[38] J. Cioslowski, E. Matito, M. Solà, *J. Phys. Chem. A* **2007**, *111*, 6521.
[39] D. W. Szczepanik, *Comput. Theor. Chem.* **2016**, *1080*, 33.
[40] D. W. Szczepanik, M. Solà, T. M. Krygowski, H. Szatylowicz, M. Andrzejak, B. Pawelek, J. Dominikowska, M. Kukulka, K. Dyduch, *Phys. Chem. Chem. Phys.* **2018**, *20*, 13430.
[41] a) P. v. R. Schleyer, C. Maerker, A. Dransfeld, H. Jiao, N. J. R. van Eikema Hommes, *J. Am. Chem. Soc.* **1996**, *118*, 6317; b) Z. Chen, C. S. Wannere, C. Corminboeuf, R. Puchta, P. v. R. Schleyer, *Chem. Rev.* **2005**, *105*, 3842; c) P. v. R. Schleyer, M. Manoharan, Z. X. Wang, B. Kiran, H. J. Jiao, R. Puchta, N. J. R. van Eikema Hommes, *Org. Lett.* **2001**, *3*, 2465; d) A. Stanger, *J. Org. Chem.* **2006**, *71*, 883.
[42] T. A. Keith, *AIMAll (Version 19.10.12)*, TK Gristmill Software, Overland Park KS, USA **2014**. http://aim.tkgristmill.com
[43] a) E. Matito, *ESI-3D: Electron sharing indexes program for 3D molecular space partitioning*. http://iqc.udg.es/~eduard/ESI, IQCC (Girona, Catalonia) and DIPC (Donostia, Euskadi), Spain **2015**; b) E. Matito, M. Solà, P. Salvador, M. Duran, *Faraday Discuss.* **2007**, *135*, 325.
[44] D. W. Szczepanik, RunEDDB (version 26-Jun-2021), Krakow, Poland, **2021**. http://www.eddb.pl/runeddb.
[45] P. Preethalayam, N. P. Vedin, S. Radenković, H. Ottosson, *J. Phys. Org. Chem.* **2022**. PMID: submitted.
[46] F. Feixas, E. Matito, J. Poater, M. Solà, *J. Phys. Chem. A* **2007**, *111*, 4513.
[47] L. Zhao, R. Grande-Aztatzi, C. Foroutan-Nejad, J. M. Ugalde, G. Frenking, *ChemistrySelect* **2017**, *2*, 863.
[48] M. Mauksch, S. B. Tsogoeva, *Chem. – Eur. J.* **2021**, *27*, 14660.
[49] M. Álvarez-Moreno, C. de Graaf, N. López, F. Maseras, J. M. Poblet, C. Bo, *J. Chem. Inf. Model.* **2015**, *55*, 95.

SUPPORTING INFORMATION

Additional supporting information can be found online in the Supporting Information section at the end of this article.

How to cite this article: S. Escayola, N. Proos Vedin, A. Poater, H. Ottosson, M. Solà, *J Phys Org Chem* **2023**, *36*(1), e4447. https://doi.org/10.1002/poc.4447